Six-Step Operation of PMSM with Instantaneous Current Control

Yong-Cheol Kwon, Sungmin Kim, *Student Member, IEEE*, and Seung-Ki Sul, *Fellow, IEEE*
School of Electric Engineering & Computer Sciences, Seoul National University, Seoul, Korea

***Abstract*—Six-step operation has many advantages on PMSM drives. Because the fundamental of inverter output is maximized by the six-step operation, capability of machine can be a lot enhanced. Furthermore, switching loss of inverter can be minimized by the six-step operation. Despite many merits of the six-step operation in AC machine drives, it was rarely adopted in dynamic applications because performance of current control is severely degraded during the six-step operation. In this paper, a control scheme for the six-step operation of PMSMs is proposed. Applying the proposed method, the six-step operation is successfully realized without losing control dynamics.**

NOMENCLATURE

Superscript "s"	stationary reference frame.
Superscript "r"	synchronously rotating rotor reference frame.
Superscript "*"	reference value.
T_e	output torque.
v_{ds}^r , v_{qs}^r	d-q components of stator voltage in rotor reference frame.
i_{ds}^r , i_{qs}^r	d-q components of phase current in rotor reference frame.
R_s	stator resistance.
L_{ds}, L_{qs}	d-q components of stator self-inductance.
ΔL	difference between d-q inductances, $L_{ds} - L_{qs}$.
ω_r	electrical speed.
λ_f	back-EMF constant.
P	number of poles.
V_{dc}	DC-link voltage.
T_{samp}	control period for current regulator.

I. INTRODUCTION

Because, back-EMF voltage is proportional to the rotational speed of motor, the output voltage of an inverter should also increase proportionally to the speed to keep the current regulation capability. However, the output voltage of the inverter is limited by DC link voltage of the inverter, which makes physical limitation of operating speed of the motor. In order to overcome the voltage constraint of PMSM (Permanent Magnet Synchronous Machine) drive system, flux-weakening control is generally used. In early researches of the flux-weakening control of PMSM [1]-[2], the voltage constraint was normally set as the inscribed circle of the voltage hexagon. With these schemes, linear region shown in Fig.1 is utilized in the steady-state and nonlinear region is utilized only in the transient-state such as rapid acceleration of the motor. Although current control dynamics is satisfactory using these methods, the capability of the inverter in the sense of the output voltage is not fully exploited in the steady-state.

Focusing on full exploitation of the output voltage capability of the inverter, six-step operation is the best method to maximize the fundamental component of the inverter output voltage in flux-weakening range. During the six-step operation, unlike normal PWM mode, only six vectors on stationary d-q voltage frame are available for the motor control. Thus in the six-step mode, voltage magnitude is fixed and only voltage angle can vary. Although the six-step operation causes sub-problems such as current harmonics, it has strong merits on AC machine drives especially in automotive application, where the torque at the higher speed is premium under the given battery voltage. Thanks to maximized inverter output voltage, torque capability and operation region of motor can be extended without any modification of hardware. Moreover, inverter switching loss can be minimized because only single switching in a fundamental period of the output voltage is needed during the six-step operation.

Although many advantages aforementioned, the six-step operation has been rarely used in PMSM drives. Because voltage magnitude is fixed and only voltage angle can be adjusted during the six-step operation, conventional PI current regulator does not work properly. So in most previous researches, the six-step operation was implemented by voltage control mode [3]-[6]. In [3]-[4], static overmodulation concept for making appropriate voltage shape in nonlinear region was proposed. In [5]-[6], six-step operation of PMSM by voltage angle control was discussed. In such voltage control approaches, only steady-state operating condition is considered and transient response of torque and current was out of interest. Inverter output voltage is produced without feedback calculation of current, thus torque control dynamics is poor. For this reason, the six-step operation was not acceptable in applications where high dynamics of torque control was required.

In order to achieve instantaneous torque control, closed loop current regulator is needed. One way to implement the six-step operation is simply saturating the current regulator [7]. Because voltage reference goes beyond the voltage hexagon, near six-step voltage can be achieved by dynamic overmodulation. But the performance of the conventional PI regulator is severely degraded in the saturated condition [8]. More consideration of the saturation of the current regulator

978-1-4673-0803-8/12/$31.00 ©2012 IEEE

is needed to keep the control performance. In [9], an algorithm for extended utilization of DC bus with instantaneous current control is proposed. Using the method in [9], the current regulator is saturated in the flux-weakening region and the inverter is operating in quasi-six-step mode. Instantaneous current control is achieved by properly modifying current reference using feedback control. However, [9] does not fully cover the six-step operation where the voltage utilization is maximized.

This paper covers a control scheme for the realization of the six-step operation of PMSM without losing current control dynamics. In the proposed method, conventional PI current regulator is operating in overall operating conditions including the six-step operation. And three control methods are devised and they are working together with the current regulator. By the proposed method, six-step operation of PMSM is successfully achieved. Because the current is controlled by the closed-loop regulator, instantaneous current control is not lost even in the six-step mode. Simulations and experiments are carried out to show the effectiveness of the proposed method.

II. Voltage Control Method for PMSM Drives

Mathematical expression of PMSM is shown in (1)-(2).

$$\begin{bmatrix} v_{ds}^r \\ v_{qs}^r \end{bmatrix} = \begin{bmatrix} R_s + sL_{ds} & -\omega_r L_{qs} \\ \omega_r L_{ds} & R_s + sL_{qs} \end{bmatrix} \begin{bmatrix} i_{ds}^r \\ i_{qs}^r \end{bmatrix} + \begin{bmatrix} 0 \\ \omega_r \lambda_f \end{bmatrix}. \quad (1)$$

$$T_e = \frac{3}{2}\frac{P}{2}\left\{\lambda_f i_{qs}^r + \Delta L \cdot i_{ds}^r i_{qs}^r\right\}. \quad (2)$$

Neglecting transient term and resistive voltage drop, steady-state current can be approximated as

$$\begin{aligned} i_{ds}^r &= \frac{v_{qs}^r}{L_{ds}\omega_r} - \frac{\lambda_f}{L_{ds}}. \\ i_{qs}^r &= -\frac{v_{ds}^r}{L_{qs}\omega_r}. \end{aligned} \quad (3)$$

Substituting (3) to (2), output torque can be deduced as

$$T_e = -\frac{3P}{4L_{ds}L_{qs}\omega_r^2}\left\{L_{qs}\omega_r\lambda_f v_{ds}^r + \Delta L v_{qs}^r v_{ds}^r\right\}. \quad (4)$$

Another way to express torque in terms of voltage magnitude and angle is

$$T_e = -\frac{3P}{8L_{ds}L_{qs}\omega_r^2}\left\{2L_{qs}\omega_r\lambda_f \cdot V\cos\theta + \Delta L \cdot V^2 \sin 2\theta\right\}. \quad (5)$$

The output torque is expressed as a function of d-q voltages or voltage magnitude and angle. Thus steady-state torque can be controlled by adjusting them [5]-[6]. However, in full expression of the torque considering all the transient terms, undesired terms arise in the torque and voltage relation. Arranging (1) according to current, following equation can be derived.

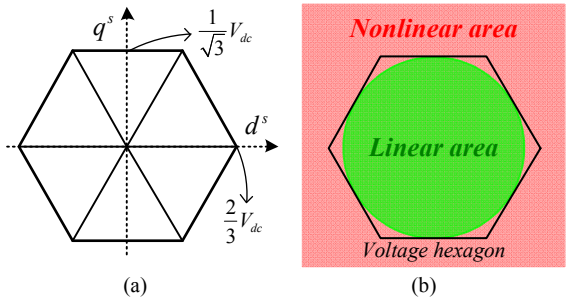

Figure 1. (a) Voltage hexagon and (b) area division.

$$\begin{bmatrix} i_{ds}^r \\ i_{qs}^r \end{bmatrix} = \frac{1}{D(s)}\begin{bmatrix} R_s + sL_{qs} & \omega_r L_{qs} \\ -\omega_r L_{ds} & R_s + sL_{ds} \end{bmatrix} \begin{bmatrix} v_{ds}^r \\ v_{qs}^r \end{bmatrix} - \frac{1}{D(s)}\begin{bmatrix} \omega_r L_{qs} \\ R_s + sL_{ds} \end{bmatrix} \omega_r \lambda_f, \quad (6)$$

where

$$D(s) = s^2 L_{ds}L_{qs} + sR_s\left(L_{ds} + L_{qs}\right) + R_s^2 + \omega_r^2 L_{ds}L_{qs}. \quad (7)$$

As shown in (6), d-q currents are expressed by second-order transfer functions from d-q voltages. For step change of input voltage, the current response is damped oscillation with exponential time constant τ expressed as

$$\tau = \frac{2L_{ds}L_{qs}}{R_s\left(L_{ds} + L_{qs}\right)} = \frac{2 \cdot L_{ds} \,||\, L_{qs}}{R_s}. \quad (8)$$

In the case of the experimental motor specified in TABLE I, τ is 26ms. This time constant causes significant time delay for settling of the current. In any operating condition for changing output torque, the transient-state lasts for at least five times of τ, 130ms. Such time delay of torque control is not acceptable in high-performance PMSM drive applications. For better dynamics of torque control, closed loop current regulator is needed.

III. Trade-Off Realation Between Steady-State Voltage Utilization and Control Dynamics

Voltage synthesis of inverter is physically confined by voltage hexagon whose magnitude depends on DC link voltage. Fig. 1(a) shows the voltage hexagon on stationary voltage plane. Only the area inside the voltage hexagon can be synthesized by inverter. Regarding to linearity of voltage synthesis, the voltage plane can be divided into linear area and nonlinear area as shown in Fig. 1(b). If the voltage reference is rotating in the linear area, inverter can linearly synthesize voltage. But if the voltage reference goes beyond the voltage hexagon, dynamic overmodulation is carried out and a point on the voltage hexagon is selected for synthesis. Fig. 2 shows voltage selection using minimum distance error overmodulation which is widely used.

As discussed in [10], the fundamental component of inverter output voltage can be increased up to $2/\pi \cdot V_{dc}$ by boosting the magnitude of the voltage reference. In the sense of fundamental voltage synthesis, the constraint of inverter output can be described as circle on synchronous

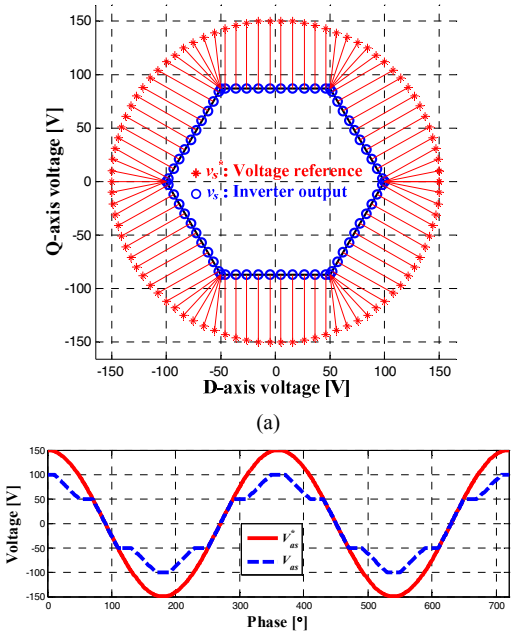

Figure 2. (a) Voltage selection and (b) phase voltage by minimum distance error overmodulation.

voltage plane. Fig. 3 shows circle constraint of inverter output, where v_s^r indicates stator voltage vector. In the figure, C_1 is the available boundary of inverter output by utilizing linear area only. C_2 is the maximum voltage boundary achieved by the six-step operation.

As expressed in (1), back-EMF is proportional to rotating speed of motor. At base speed, the magnitude of back-EMF reaches near the limit of the inverter capacity. Then flux-weakening control for higher speed operation is required to keep the current regulation capability. The role of flux-weakening controller is to determine operating current satisfying current and voltage constrains as follows:

$$\begin{aligned} i_{ds}^{r\,2} + i_{qs}^{r\,2} &\le I_{\lim}{}^2. \\ v_{ds}^{r\,2} + v_{qs}^{r\,2} &\le V_{\lim}{}^2. \end{aligned} \tag{9}$$

The current limit $I_{\lim}$ is normally determined by thermal capacity of motor drive system. $V_{\lim}$ is a target value for controlling the magnitude of steady-state terminal voltage as constant in flux-weakening region.

The setting of $V_{\lim}$ is very tricky because it determines trade-off relation between steady-state voltage utilization and dynamic performance of current control. $V_{\lim}$ is commonly set to be lower than $1/\sqrt{3}\cdot V_{dc}$. Then steady-state back-EMF is controlled to be inside C_1 and the linear area is utilized. The area between C_1 and C_2 is utilized only in dynamic condition. For example, if step command for increasing torque is applied, voltage reference temporarily

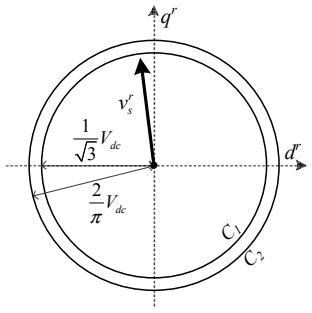

Figure 3. Circle constraint of inverter output.

goes inside the nonlinear area and dynamic overmodulation is carried out. Because the nonlinear area is reserved as a voltage margin, current control dynamics is quite satisfactory [8].

If $V_{\lim}$ is set to be between $1/\sqrt{3}\cdot V_{dc}$ and $2/\pi\cdot V_{dc}$ [9], back-EMF is located between C_1 and C_2 and nonlinear area is utilized even in steady-state. Although steady-state voltage utilization increases, voltage margin for current control becomes relatively deficient. As a result, current control dynamics is significantly degraded.

The six-step operation is an extreme case for voltage utilization. $V_{\lim}$ is set as $2/\pi\cdot V_{dc}$ and inverter output is on C_2 in steady-state operating condition. Because inverter output is already maximized in the steady-state, there is no voltage margin reserved for transient-state current control. In other word, there is no way to increase the output voltage of the inverter even for very short time. For this reason, degradation of current control performance is inevitable.

IV. Proposed Scheme

Fig. 4 shows block diagram of proposed PMSM drive system. In the drive system, three controllers, Part I, Part II, and Part III, are devised and added. Each of the three controllers serves a critical role for the six-step operation of PMSM. The three controllers are explained one by one in this chapter.

A. Part I: Dynamic Overmodulation for Six-Step Operation

Because closed-loop current regulator is used in Fig. 4, the voltage reference is produced by the regulator. So it is impossible to directly feed six-step voltage to the motor. In the proposed scheme, the six-step voltage is produced by dynamic overmodulation. Letting the voltage reference rotate outside the voltage hexagon in the flux-weakening region, dynamic overmodulation is continuously carried out. Fig. 5 shows a dynamic overmodulation method devised especially for the six-step voltage generation. The criterion of voltage selection is very simple: Whenever the voltage reference goes beyond the voltage hexagon, a corner of the voltage hexagon which is nearest to the voltage reference is selected for inverter output. As shown in Fig. 5(b), perfect six-step voltage can be generated by Part I.

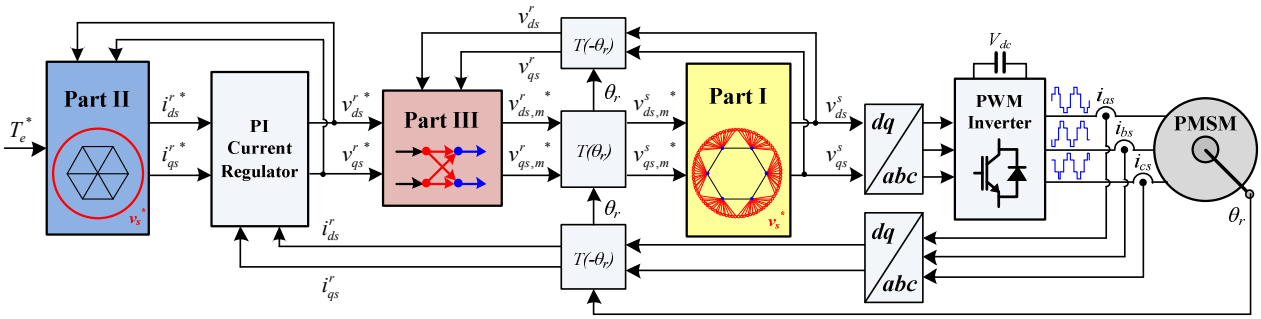

Figure 4. Block diagram of proposed drive system for six-step operation of PMSM.

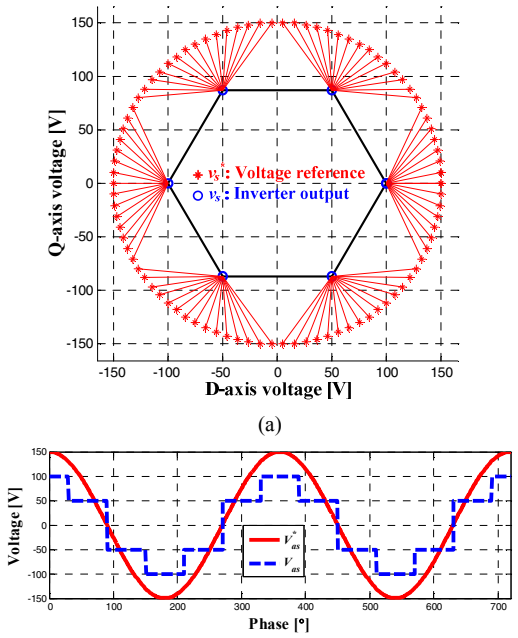

Figure 5. (a) Voltage selection and (b) phase voltage by Part I.

B. Part II: Flux-Weakening Controller

Two constraints in (9) can be graphically expressed as Fig. 6. Voltage constraint is expressed as an ellipse and current constraints is expressed as a circle on current plane [1]. Because both constraints should be satisfied, operating current is always located inside the intersection area between voltage and current constraints.

Under the assumption that the current reference is at point A in Fig. 6, then the current at A can be realized by the current regulator because A is in the intersection area. If the torque command is applied in this condition, then the current reference moves to point B. Because B does not satisfy voltage constraints denoted by ellipse in Fig. 6, the actual current cannot reach point B. In this condition, steady-state error of current is continuously integrated by PI current regulator and makes the voltage reference goes to infinity. To cope with this problem, a scheme of the flux weakening

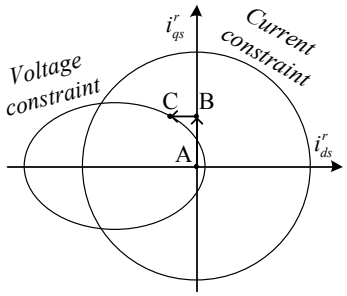

Figure 6. Voltage and current constraints on current plane.

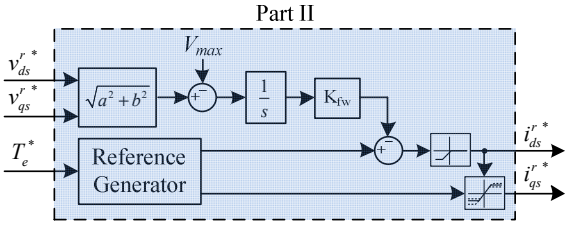

Figure 7. Structure of Part II.

control should be engaged and the scheme makes the reference B move to a feasible point C.

Because equation based feed-forwarding methods [1] are weak at parameter variation, feedback based methods [2], [9] are adopted in Part II. Fig. 7 shows the control algorithm of Part II, where V_{max} means the radius of the voltage reference during the six-step operation. With given current reference from the reference generator, integrator modifies d-axis current reference. The saturation block for q-axis current reference limits i_{qs}^{r*} by upper and lower boundaries as

$$-\sqrt{I_{\lim}{}^2 - i_{ds}^{r*2}} \le i_{qs}^{r*} \le \sqrt{I_{\lim}{}^2 - i_{ds}^{r*2}}. \qquad (10)$$

If initial current reference is at point B, the integrator operates until the reference goes to C and the current error diminishes.

C. Part III: Voltage Reference Modification for Improved Control Dynamics

As explained in chapter III, instantaneous current control is very difficult during the six-step operation due to

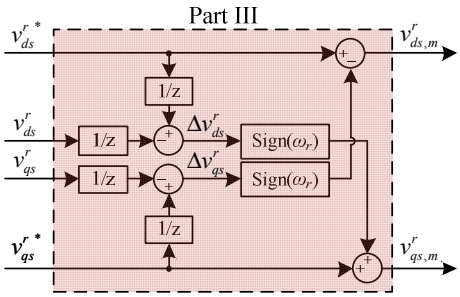

Figure 8. Structure of Part III.

absolutely no voltage margin. The role of Part III is increasing dynamic performance of current control in this situation. The key idea of Part III comes from [8]. Neglecting resistive voltage drop, the voltage equation can be written as

$$\begin{aligned} sL_{ds}i_{ds}^{r} &= v_{ds}^{r} - e_{ds}^{r}. \\ sL_{qs}i_{qs}^{r} &= v_{qs}^{r} - e_{qs}^{r}. \end{aligned} \tag{11}$$

$$\begin{aligned} e_{ds}^{r} &= -\omega_{r}L_{qs}i_{qs}^{r}. \\ e_{qs}^{r} &= \omega_{r}(L_{ds}i_{ds}^{r} + \lambda_{f}). \end{aligned} \tag{12}$$

In (12), e_{ds}^{r} and e_{qs}^{r} are d-q components of effective back-EMF which come from the rotation of the motor. Equation (11) implies that the slope of current is determined by the deviation between terminal voltage and effective back-EMF. When the output toque of the motor should be increased rapidly, then as seen from (11) there should be a large gap between v_{qs}^{r} and e_{qs}^{r} to increase q-axis current, which generates torque of the motor. Considering that the magnitude of terminal voltage is fixed during the six-step operation, the only way to increase the gap between v_{qs}^{r} and e_{qs}^{r} is reducing e_{qs}^{r}. As seen from (12), e_{qs}^{r} can be reduced by decreasing i_{ds}^{r}, Part III temporarily decreases i_{ds}^{r} to increase i_{qs}^{r}. In the same way, i_{qs}^{r} is temporarily increased when i_{ds}^{r} should increase.

Fig. 8 shows the structure of Part III. Part III is closely related with proportional controller in the current regulator. For example, if q-axis current reference is increased in a step manner, current error Δi_{qs}^{r} is directly reflected to the voltage reference by the proportional controller. Then a large magnitude of Δv_{qs}^{r} is generated and subtracted from d-axis voltage reference. As the result, d-axis current rapidly decreases and q-axis current increases fast. In the same way, Δv_{qs}^{r} is added to d-axis voltage reference and make q-axis current increase rapidly. Since Part III operates only when the voltage reference is outside the voltage hexagon, it does not influence steady-state operation under the base speed.

Fig. 9 describes how the voltage vector is modified by Part III. In the figure, the voltage hexagon is approximated as a circle with radius $2/\pi \cdot V_{dc}$. Voltage reference $v_{s}^{r*}[n_1]$ in the first step is finally modified to $v_{s,m}^{r*}[n_3]$ in the third step and actual inverter output is changed from $v_{s}^{r}[n_1]$ to $v_{s}^{r}[n_3]$. Part III finds out better voltage for the current control at every control period and the voltage reference is continuously adjusted during the six-step operation.

V. Simulation Results

In all simulations, settings and parameters in TABLE I are used. Three conditions are simulated by Matlab Simulink.

A. Condition 1: Performance Evaluation of Part III

This condition is designed to evaluate the effectiveness of Part III only without Part I and Part II. So the Part II is taken out and Part I is replaced by conventional minimum distance overmodulation method. Holding speed at 750r/min, maximum torque command is applied. Fig. 10 shows simulation results. In the figure, (a)-(b) are current behaviors and (c)-(d) show voltage trajectory on d-q plane. In Fig. 10(a), settling time of current is 11ms. However, the settling time is reduced to 7ms by Part III as shown in Fig. 10(b). This 36% improvement in settling time comes from the voltage modification. Fig. 10(d) shows how the voltage reference is modified. When the voltage reference goes beyond the voltage hexagon, Part III starts to operate and rapidly modifies the voltage reference. It is notable that d-axis current is temporarily decreased by this voltage modification.

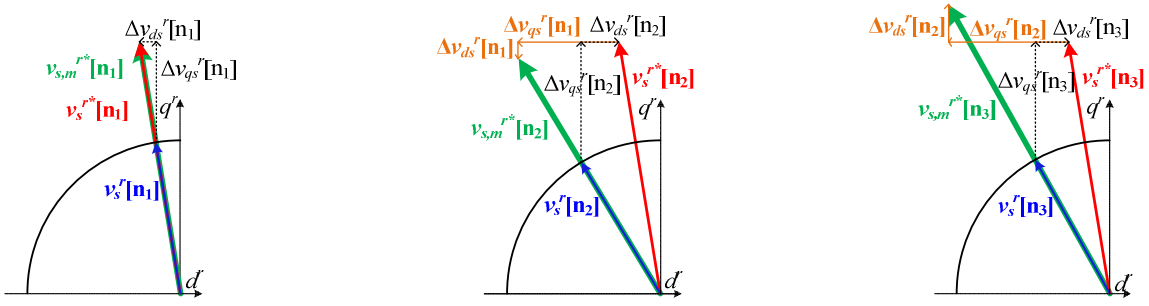

(a) First control step (n_1). (b) Second control step (n_2). (c) Third control step (n_3).

Figure 9. Adjustment of voltage reference by Part III.

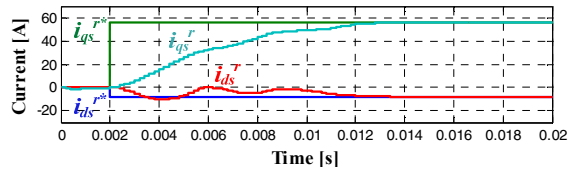

(a) Current waveform without Part III.

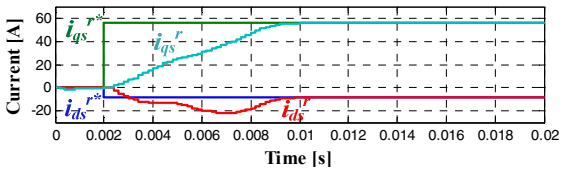

(b) Current waveform with Part III.

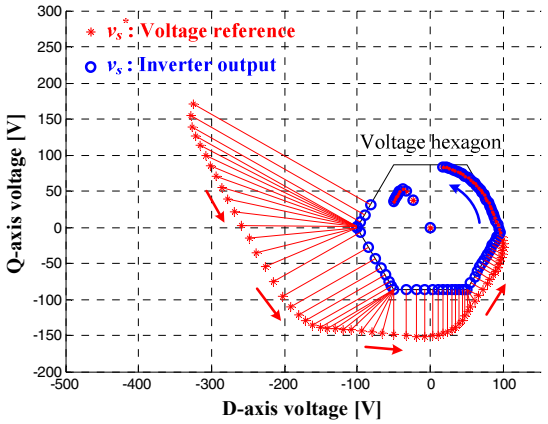

(c) Voltage trajectory without Part III.

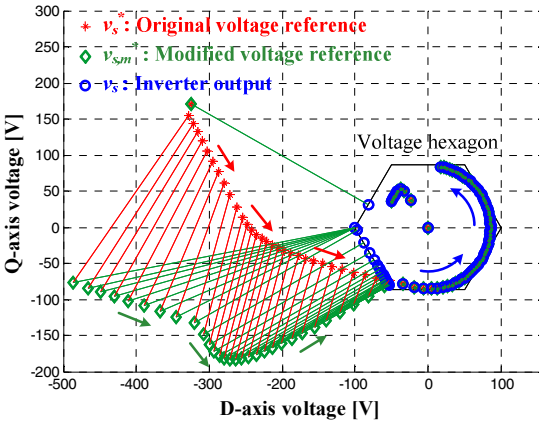

(d) Voltage trajectory with Part III.

Figure 10. Simulation results in condition 1.

B. *Condition 2: Transition Between SVPWM and Six-Step Mode*

Mode transition between SVPWM and six-step mode is simulated. Holding speed at 1000r/min, maximum torque command is applied from 0.1s to 0.3s. Fig. 11 shows the results. From 0s to 0.1s, the current reference satisfies both current and voltage constraints and SVPWM is used for the current control. From 0.1s to 0.3s, the current reference initially moves to unfeasible area and is pushed to feasible area by flux-weakening controller. In this period, the current is rapidly regulated under the six-step operation. From 0.3s to 0.5s, the current is changed back to the original value and SVPWM is activated again. Fig. 12 shows voltage trajectory from 0.11s to 0.3 when the six-step operation is activated. At every cycle of rotation, voltage reference is successively adjusted by Part III.

C. *Condition 3: Comparison of Voltage Angle Control and Proposed Method*

In this condition, step responses of the voltage angle control method and the proposed method are compared. Holding speed at 1500r/min, maximum torque command is applied from 0.1s to 0.3s in a step manner. Fig. 13 shows the results. In the figure, (a) is result from the voltage angle control. From the steady-state torque equation (5), voltage angle is controlled to control the torque. Although steady state torque can be controlled, undesirable oscillation occurs in the current response. The amplitude of the oscillating component is exponentially decaying with time constant τ expressed in (8). Due to this oscillation, settling time for current is more than 130ms. Fig. 13(b) is the result from the proposed method. Q-axis current is well regulated in 10ms when increasing torque. Although d-axis current has relatively long settling time, it doesn't contribute much to the output torque.

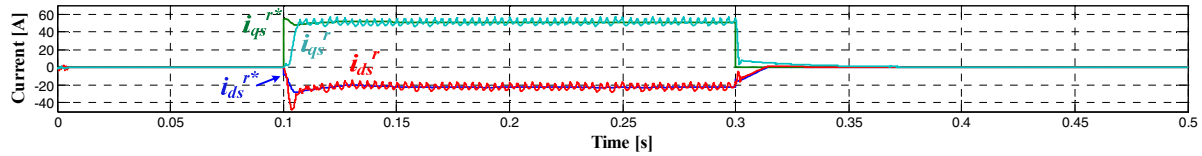

(a) Current waveform.

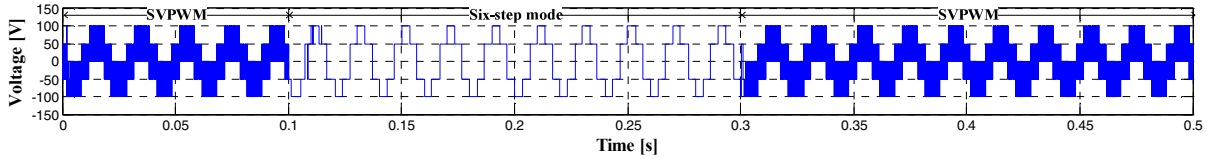

(b) Voltage waveform.

Figure 11. Simulation results in condition 2.

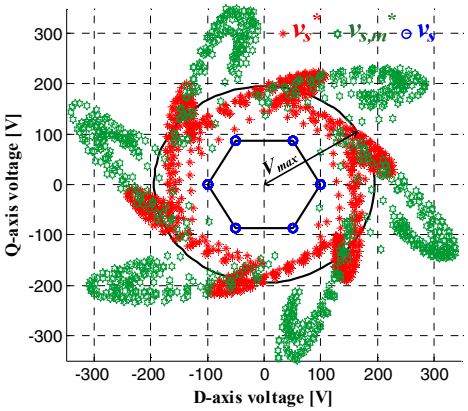

Figure 12. Voltage trajectory during the six-step operation.

VI. EXPERIMENTAL RESULTS

Experimental settings and parameters are specified in TABLE I. Fig. 14 shows the experimental set-up. Several tests are done to verify the effectiveness of the proposed method and the results are compared to the simulation results in previous chapter.

A. Test 1

The experimental test condition is the same as the simulation condition 2. Speed is held at 1000r/min by the loads machine, maximum torque command is applied from 0.1s to 0.3s. Experimental waveforms in Fig 15 well match to the simulation waveforms in Fig.11. Seamless transition between SVPWM and the six-step mode is realized by the proposed method.

B. Test 2

The condition of this test is the same as simulation condition 3. Speed is fixed at 1500r/min and maximum torque command is applied from 0.1s to 0.3s. Experimental waveforms in Fig 16 match to the simulation waveforms in Fig. 13(b). Because flux weakening control is needed at 1500r/min even in zero torque command condition, the six-step mode is activated in from 0s to 0.5s except in transient period from 0.3s to 0.37s where the voltage command goes inside the linear area for decreasing torque.

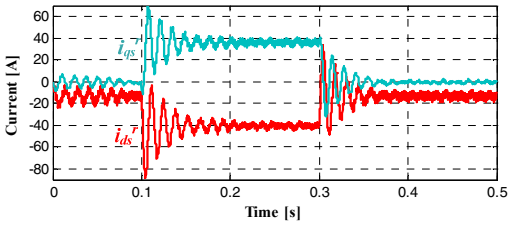

(a) Current waveform from voltage angle control.

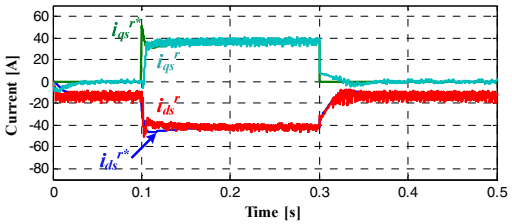

(b) Current waveform from proposed method.

Figure 13. Simulation results in condition 3.

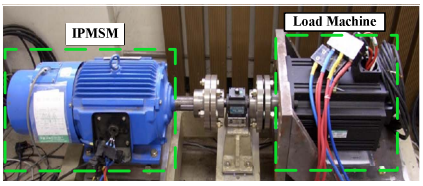

Figure 14. Experimental set-up.

C. Test 3

In this test, steady state torque is measured from zero speed to 2500r/min experimentally. The conventional scheme indicates the scheme only utilizing the linear region [2] in the flux-weakening region. The results are shown in Fig. 17. By the six-step operation, maximum torque capability of PMSM is achieved. As shown in Fig. 17(a), from 900r/min to 2500r/min, the flux weakening region, the output torque is enhanced by more than 17%. The base speed is changed from 715r/min to 840r/min, which means extended constant torque region by 17%. And, as seen from Fig. 17(b), the power capability of the motor under the same current and voltage constraints has been enhanced by 25% at 2500 r/min.

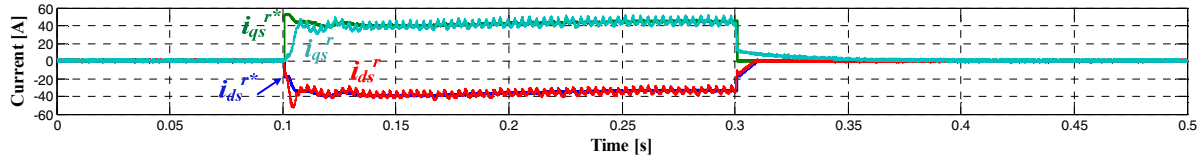

(a) Current waveform.

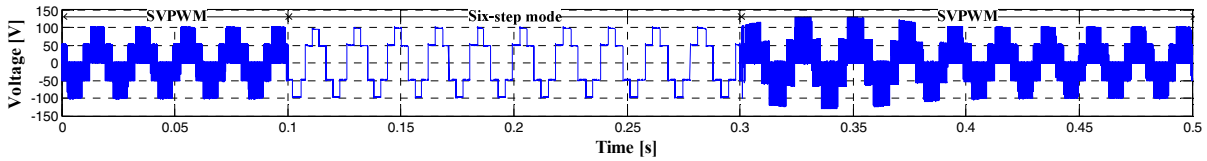

(b) Voltage waveform.

Figure 15. Experimental test 1.

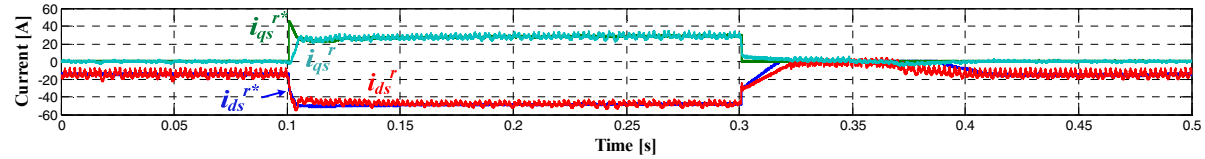

(a) Current waveform.

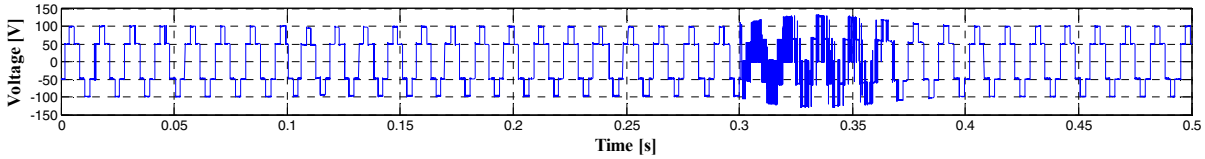

(b) Voltage waveform.

Figure 16. Experimental test 2.

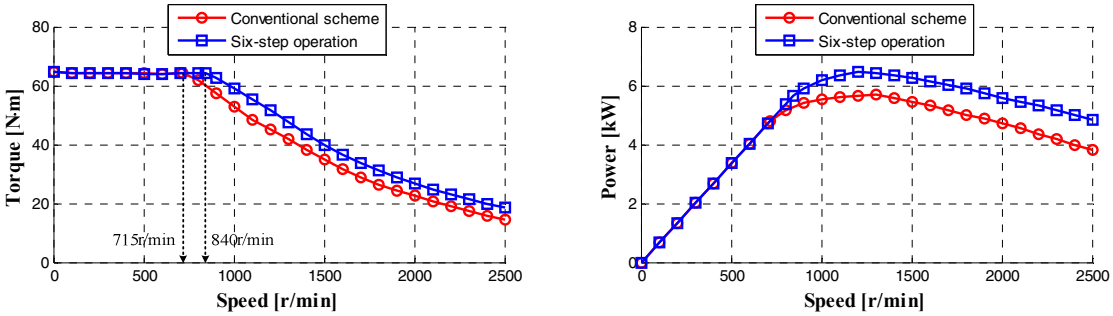

(a) Torque vs speed curve.

(b) Power vs speed curve.

Figure 17. Capability curves.

VII. CONCLUSIONS

This paper covers investigations and realization of the six-step operation of PMSM. Applying the proposed method, the capability of PMSM can be enhanced up to the real physical limit. Furthermore, the instantaneous current control is successfully achieved even in such condition that the torque command rapidly changes. Computer simulation and experimental results support the validity of the proposed method. The output torque capability has been enhanced by 17% and the constant torque region is extended by 17%. And a quarter of more power is available at 2500 r/min under the same voltage and current constraints. Regardless of these enhancements, the dynamic performance of the current regulation has been kept due to collaborated functioning of the devised three controllers.

APPENDIX

TABLE I. EXPERIMENTAL SETTING AND PARAMETERS

T_{samp}	100μs	R_s	0.15Ω
V_{dc}	150V	λ_f	0.254V·s
Rated current	39.5A_{rms}	L_{ds}	3.6mH
P	6 poles	L_{qs}	4.3mH

REFERENCES

[1] S. Morimoto, Y. Takeda, and T. Hirasa, "Expansion of operating limits for permanent magnet motor by current vector control considering inverter capacity," IEEE Trans. Ind. Appl., vol. 26, no. 5, pp. 866-871, Sept./Oct. 1990.

[2] J. M. Kim and S. K. Sul, "Speed control of interior permanent magnet Synchronous motor drive for the flux weakening operation," IEEE Trans. Ind. Appl., vol. 33, no. 1, pp. 43-48, Jan./Feb. 1997.

[3] J. Holtz, W. Lotzkat, and M. Khambadkone, "On continuous control of PWM inverters in the overmodulation range including the six-step mode," IEEE Trans. Power Electron., vol. 8, no. 4, pp. 546–553, Oct. 1993.

[4] D. C. Lee and G. M. Lee, "A novel overmodulation technique for space-vector PWM inverters," IEEE Trans. Power Electron., vol. 13, no. 6, pp. 1144–1151, Nov. 1998.

[5] R. Monajemy and R. Krishnan, "Performance comparison for six-step voltage and constant back EMF control strategies for PMSM," 34th IAS Annual Meeting. Conference Record of the 1999 IEEE , vol.1, no., pp. 165-172.

[6] K. Asano, Y. Inaguma, H. Ohtani1 E. Sato, M. Okamura and S. Sasaki, "High Performance Motor Drive Technologies for Hybrid Vehicles," Proceeding of PCC-Nagoya 2007, pp.1584-1589, 2007.

[7] T. M. Jahns, G. B. Kliman, and T. W. Neuman, "Interior PM synchronous motors for adjustable speed drives," IEEE Trans. Ind. Appl., vol. IA-22, no. 4, pp. 738–747, July/Aug. 1986.

[8] Y. C. Kwon, S. Kim, and S. K. Sul, "Voltage feedback current control scheme for improved transient performance of permanent magnet synchronous machine drives," IEEE Trans. Ind. Electron., vol. 59, no. 9, pp. 3373-3382, Sept. 2012.

[9] T. S. Kwon and S. K. Sul, "Novel antiwindup of a current regulator of a surface-mounted permanent-magnet motor for flux-weakening control," IEEE Trans. Ind. Appl., vol. 42, no. 5, pp. 1293-1300, Sept./Oct. 2006.

[10] A. M. Hava, R. J. Kerkman, T. A. Lipo, "Carrier-based PWM-VSI overmodulation strategies Analysis, comparison, and design," IEEE Trans. Power Electron., vol. 13, no. 4, pp. 674–689, July 1998.